

Classical Coulomb blockade of a silicon nanowire dot

Shaoyun Huang,¹ Naoki Fukata,^{2,3} Maki Shimizu,^{1,4} Tomohiro Yamaguchi,¹ Takashi Sekiguchi,⁵ and Koji Ishibashi^{1,a)}

¹Advanced Device Laboratory, RIKEN, 2-1, Hirosawa, Wako, Saitama 351-0198, Japan

²International Center for Materials Nanoarchitectonics, National Institute for Materials Science, 1-1 Namiki, Tsukuba 305-0044, Japan

³PRESTO, Japan Science and Technology Agency, 4-1-8 Honcho Kawaguchi, Saitama 332-0012, Japan

⁴Department of Physics, Tokyo University of Science, 1-3, Kagurazaka, Shinjuku-ku, Tokyo 162-8601, Japan

⁵Advanced Electronic Materials Center, National Institute for Materials Science, 1-1 Namiki, Tsukuba 305-0044, Japan

(Received 21 March 2008; accepted 6 May 2008; published online 28 May 2008)

Single electron transistors (SETs) have been fabricated with an individual *n*-type single-crystal silicon nanowire (SiNW) that was grown by a catalytic chemical vapor deposition technique, and their transport properties have been measured in low temperatures. The SiNW-SET in the present work exhibited well pronounced Coulomb oscillations in a wide gate voltage range from -10 to 10 V, featuring in uniform peak height, uniform full width at half maximum, and equidistant peak spacing. The charging energy turned out to be $64 \mu\text{eV}$. The temperature dependence of Coulomb oscillations revealed that the dot worked within the classical Coulomb blockade model.

© 2008 American Institute of Physics. [DOI: 10.1063/1.2937406]

Recently, silicon nanowires (SiNWs) with a diameter of a few tens of nanometers have been produced with a catalytic chemical vapor deposition technique. These SiNWs with the diameters that are difficult to realize with conventional lithography techniques could be attractive building blocks for extremely small quantum-dot based nanodevices and have stimulated extensive interest in the past years.^{1,2} Compared with other self-assembled one-dimensional materials, e.g., carbon nanotubes,³ SiNWs allow us to use matured Si fabrication processes, which enhances reliability and reproducibility of the fabricated devices. A long spin coherence time, due to the small spin-orbit interaction and the small hyperfine interaction, has been predicted⁴ and experimentally demonstrated⁵ in recent works. These facts suggest that the Si-quantum dot could be a promising candidate for spin based quantum computing devices.⁶ As the first step toward the direction, to precisely control a charge and a spin on a single-electron level is necessary, and can be done with a single electron transistor (SET). In the past decades, the SETs have been fabricated in a wide variety of Si nanostructures, such as those fabricated by a top-down approach of Si-on-insulator substrates^{7,8} and those fabricated with a bottom-up approach using nanocrystals.⁹ The former takes advantage of the self-limited oxidation mechanism to reduce the dot size, but the formed tunneling barriers as well as the dot size are hard to control. The latter provides high quality nanoscale Si crystals, but fabricating reliable contacts to them still remains a big challenge. Until now, most of the demonstrated devices with SiNWs are field-effect transistors with switching functions.¹⁰ Few works, however, achieved a SiNW-SET although there is a work on *p*-type SiNW-SETs.¹¹ The present work reports on the realization of *n*-type SiNW-SETs, and shows that the fabricated SET with a relatively

large diameter exhibits classical Coulomb blockade behaviors with uniform Coulomb oscillations.

Intrinsic single-crystal SiNWs with diameters of $40\text{--}70$ nm and lengths around $1 \mu\text{m}$ were synthesized via the gold nanocatalysts mediated vapor-liquid-solid mechanism in the silane chemical-vapor-deposition (CVD) at 550°C for 4 h. A typical SiNW with a diameter of 50 nm and a length of $1.4 \mu\text{m}$ is shown in Fig. 1(a). The high resolution transmission-electron-microscope (HRTEM) observation reveals that the SiNW is a single crystal with a $\langle 111 \rangle$ orientation along the growth direction, as shown in Fig. 1(b). Subsequently, the as-prepared SiNWs were highly doped with phosphorus dopants in a furnace to define the carrier type as well as to increase the carrier density to

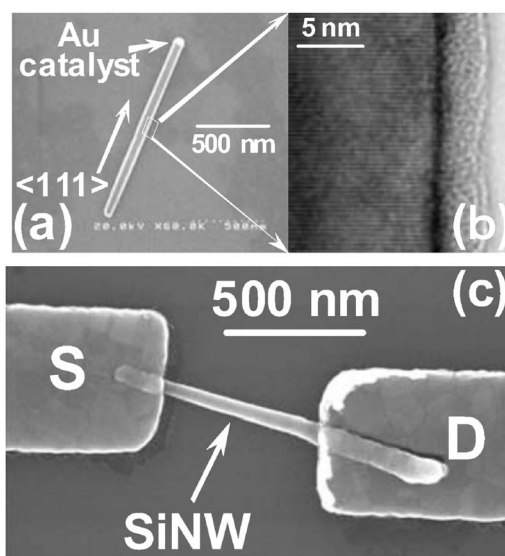


FIG. 1. (a) SEM image of a dispersed SiNW with a diameter of 60 nm and length of $1.4 \mu\text{m}$. (b) HRTEM image of the SiNW. (c) SEM image of a typical device. The source/drain electrodes were fabricated with Ni(150 nm)/Au(50 nm) by electron-beam evaporation method.

^{a)} Author to whom correspondence should be addressed. Present Address: Advanced Device Laboratory, RIKEN, 2-1, Hirosawa, Wako, Saitama 351-0198, Japan. Tel.: +81-48-5734-2542. FAX: +81-48-462-4659. Electronic mail: kishiba@riken.jp.

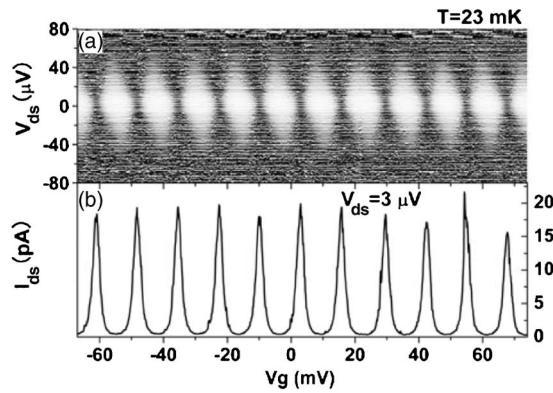


FIG. 2. (a) Stability diagram of the SET. Within the diamonds, Coulomb blockade is established, while outside, a current flows across the SiNW. (b) The corresponding Coulomb oscillations with back-gate voltages from -67 to 74 mV at the fixed source-drain bias of $3 \mu\text{V}$. Coulomb peaks occur at gate voltages where two adjacent diamonds meet.

10^{18} – 10^{19} cm^{-3} to allow low temperature transport measurements. The n -type SiNWs were, then, suspended in ethanol solution and transferred onto a surface oxidized Si substrate by the drop-coating method. To examine the extreme dimension for feasible SiNW-SET operations, we chose a SiNW with a diameter of 70 nm and a length of $1 \mu\text{m}$ for Coulomb island (dot) fabrication. As shown in Fig. 1(c), source and drain contacts were fabricated on an individual SiNW by using electron-beam lithography, metal evaporation and lift-off techniques. A highly Sb-doped n -type Si with a thermally grown 200 nm SiO_2 layer was used for a substrate. The top SiO_2 layer isolates individual SiNWs from each other and allows the use of the substrate for back gating.

The source and drain contacts (also called leads) are made of Nickel with a thickness of 150 nm , and have a separation of 450 nm . These metal-semiconductor contacts produce Schottky barriers at the SiNW surface with a height of 400 meV .¹² A depletion layer in the SiNW can be roughly estimated to be 20 nm , based on the plausible doping concentration. The Schottky barriers, therefore, work as the double tunnel barriers to confine electrons in the isolated SiNW. A part of the SiNW underneath the metal leads may not be completely depleted, so that, for the present sample, a whole SiNW could be a Coulomb island with possible reduction underneath the leads. The sample was set on the mixing chamber in a dilution refrigerator with low-pass filters in each lead at the lowest temperature, to prevent high frequency noise that may come from higher temperatures. Then, single-electron transport properties through the SiNW-SET were investigated by measuring a current (I_{ds}) as functions of the back-gate voltage (V_g) and the source-drain voltage (V_{ds}).

In the linear response regime with a small V_{ds} , the number of electrons in the dot can be controlled on the single-electron level. Increasing the gate voltage populates the dot with electrons, by pulling down its potential with respect to the Fermi energy of the leads. Whenever an additional electron state in the dot comes in the bias window set by V_{ds} , Coulomb blockade is lifted, resulting in a sudden increase in the current through the dot. Indeed, at 23 mK of the mixing-chamber temperature (T_s), the pronounced Coulomb oscillations of I_{ds} were observed, as shown in Fig. 2(b), when the V_{ds} was biased at $3 \mu\text{V}$. It is worthwhile to point out that the T_s may not necessarily be same with the electron temperature (T) which can be derived from the Coulomb oscillation

peaks (see later). The current is thus due to electrons tunneling from one lead into the dot, and out of the dot to the other lead one by one. Every current peak originates from correlated single-electron tunneling events between N and $N+1$ states, vice versa. In between the Coulomb peaks, the current is dramatically suppressed, the Coulomb blockade effect.¹³ The peak to valley ratio is well over two orders of magnitude and is noise limited. When the back-gate voltage was swept from -10 to 10 V , the successive Coulomb peaks were observed, indicating more than thousand of electrons to be counted and controlled. All of the Coulomb peaks feature in the uniform peak height, uniform full width at half maximum (FWHM), and equidistant spacing in V_g . These features in Coulomb oscillations are similar to those in the metallic SET,¹⁴ in contrast to small semiconductor quantum dots¹⁵ and the carbon nanotube quantum dots,¹⁶ where each peak height varies very much, and the peak spacing is not uniform due to pronounced quantum confined levels.

A charge stability diagram around the zero back-gate voltage (V_g) is shown in Fig. 2(a), where the differential conductance ($dI_{\text{ds}}/dV_{\text{ds}}$) is plotted in a gray scale manner as functions of V_g and V_{ds} . The diamond shaped white regions are so called Coulomb diamonds in which the current is suppressed. It should be noted that the current peaks in Fig. 2(b) occur at the gate voltages where two adjacent diamonds meet in Fig. 2(a). From the dimensions of the Coulomb diamonds, the self-capacitance (C_Σ) and the gate capacitance (C_g) are obtained to be 2.5 fF and 12.3 aF , respectively. The gate conversion factor $\alpha \equiv C_g/C_\Sigma$ is calculated to be 4.9×10^{-3} . From the slopes of the diamond boundaries, the source and drain capacitances (C_s and C_d) are obtained to be 1.5 and 1.0 fF , respectively. These experimentally obtained C_s , C_d , and C_g contribute to C_Σ by $C_\Sigma = C_s + C_d + C_g$, which agrees well with the experimentally obtained C_Σ . The charging energy $E_c = e^2/C_\Sigma$ turns out to be $64 \mu\text{eV}$, where e is the elementary charge. Because of the relatively large C_s and C_d , the observed E_c is much smaller than that of reported Si SETs. However, the E_c of the SiNW-SET could be increased up to tens of meV by sophisticated lead configurations and by shrinking the diameter of the SiNW (D) because (1) the self-capacitance of the SiNW dot increases with D^2 and (2) the complete depletion in the SiNW underneath the metal leads would reduce the effective channel length.

To further derive the nature of the SiNW-SET, temperature dependence of the Coulomb oscillations was examined from 23 to 250 mK of the T_s . The results are shown in Fig. 3, where the conductance (G) is normalized by the conductance peak height (G_{max}). Experimentally, the Coulomb oscillations were observable up to $\sim 400 \text{ mK}$. It can be seen that increasing the temperature broadens the peak width, but the Coulomb oscillation peaks do not change their positions and heights. On the contrary, the conductance between the neighboring peaks rises as the temperature is increased. Those suggest that the SiNW dot is in the classical Coulomb blockade regime, i.e., $h\Gamma_{s(d)}, \Delta \ll k_B T \ll E_c$, where h and k_B are the Planck constant and the Boltzmann constant, respectively, while Δ is an average spacing among discrete energy levels of the dot and is much smaller than $k_B T$ and E_c . The Γ_s/Γ_d are the tunneling rates at the source/drain, and usually varies substantially from level to level for small semiconductor quantum dots with a few electrons¹⁵ and for carbon nanotube quantum dots,¹⁶ which leads to a large variation in

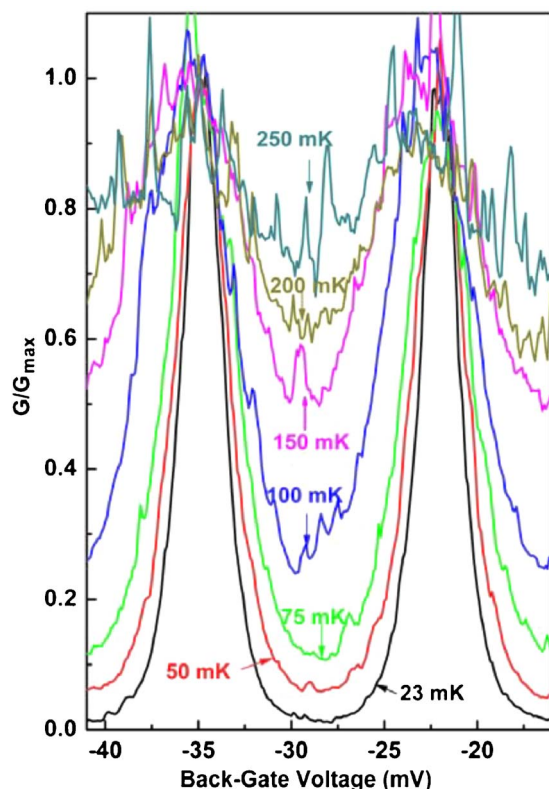


FIG. 3. (Color online) Coulomb peaks at different temperatures at a source-drain bias of $3 \mu\text{V}$. The conductance is normalized with the conductance peak height (G_{max}). Temperatures indicated here are the mixing-chamber temperatures.

Coulomb peak heights. However, as seen in Fig. 2(b), the peak heights of the present device are uniform, suggesting the uniform Γ_s/Γ_d as a function of energy. This may be because the present SiNW is highly degenerated with many electrons in a conduction band, as is the case for metallic dots, and may have a uniform density of states with negligible energy dependence. In our device, the Γ_s/Γ_d are determined by the Schottky barriers at the SiNW surface, and turn out to be extremely small owing to the finite Schottky barrier height and the depletion layer. For a rough order estimate for the single electron transport with $I=e\Gamma$, they are of the order of $10^8 \text{ (s}^{-1}\text{)}$. As a consequence, the $\hbar\Gamma_{s(d)}$, a finite width of energy levels in the dot, is small enough to avoid quantum fluctuation of charges.

The present SiNW dot is in the classical regime as indicated before, and the conductance in this regime is described as^{17,18}

$$\frac{G}{G_{\text{max}}} = \frac{\delta/k_B T}{2 \sinh(\delta/k_B T)}, \quad (1)$$

$$G_{\text{max}} = \frac{e^2 D_{\text{dot}}}{2} \frac{\Gamma_s \Gamma_d}{\Gamma_s + \Gamma_d}, \quad (2)$$

$$\delta = e\alpha |V_p - V_g|, \quad \alpha = \frac{C_g}{C_\Sigma}, \quad (3)$$

where D_{dot} and V_p are the density of states in the dot and the gate voltage at the conductance peak, respectively. The model describes that the conductance peak height is determined by the D_{dot} and Γ_s/Γ_d , while the conductance in the valley is determined by the thermal activation over the

Coulomb blockade. The FWHM depends on the temperature as $4.35k_B T/\alpha e$, but is V_g independent. The electron temperature in the leads can be obtained by fitting the Coulomb oscillation peaks with the Eq. (1), which gives 34 mK. This number happens to be as close as T_s of 23 mK. The fitting used the α parameter which was independently obtained from the stability diagram in Fig. 2(b), while the V_p was automatically modified to be consistent with the experimental one. As the temperature is increased, the thermal energy becomes close to the charging energy, so that the fitting with the Eq. (1) is not applicable any more.

So far, these experiments have been carried out at milli-Kelvin temperatures, but the prospective operation temperature of SiNW-SETs could be increased remarkably when the diameter of SiNWs is miniaturized to several nanometers. In this case, the SiNW underneath the contacts would be completely depleted, leaving the SiNW between the contacts much smaller. Accordingly, the SiNW-dot could be modeled by the one-dimensional hard-wall potential with pronounced quantized energy levels. The Coulomb island, hence, would be treated as a quantum dot.

In summary, a *n*-type single-crystal SiNW-SET was fabricated with a chemically bottom-up method and its single electron transport properties were characterized at low temperatures. The present SiNW-SET had dimensions of 70 nm in diameter and $1 \mu\text{m}$ in length, and exhibited well pronounced classical Coulomb-blockade characteristics with the charging energy of $64 \mu\text{eV}$. The Coulomb-oscillation peaks had uniform peak shapes with temperature-independent peak heights. These results open a new path to build a quantum dot with the *n*-type SiNWs by minimizing the diameter below 70 nm.

The authors acknowledge Professor Shunri Oda of Tokyo Institute of Technology for providing us with a doping source.

¹Y. Huang, X. Duan, Y. Cui, L. J. Lauhon, K.-H. Kim, and C. M. Lieber, *Science* **294**, 1313 (2001).

²N. Fukata, T. Oshima, N. Okada, K. Murakami, T. Kizuka, T. Tsurui, and S. Ito, *J. Appl. Phys.* **100**, 024311 (2006).

³K. Ishibashi, S. Moriyama, D. Tsuya, T. Fuse, and M. Suzuki, *J. Vac. Sci. Technol. A* **24**, 1349 (2006).

⁴C. Tahan and R. Joynt, *Phys. Rev. B* **71**, 075315 (2005).

⁵S. D. Sarma, R. D. Sousa, X. Hu, and B. Koiller, *Solid State Commun.* **133**, 737 (2005).

⁶D. Loss and D. P. Divincenzo, *Phys. Rev. A* **57**, 120 (1998).

⁷Y. Takahashi, M. Nagase, H. Namatsu, K. Kurihara, K. Iwade, K. Nakajima, S. Horiguchi, K. Murase, and M. Tabe, *Electron. Lett.* **31**, 136 (1995).

⁸J. Gorman, D. G. Hasko, and D. A. Williams, *Phys. Rev. Lett.* **95**, 090502 (2005).

⁹A. Dutta, S. Oda, Y. Fu, and M. Willander, *Jpn. J. Appl. Phys., Part 1* **39**, 4647 (2000).

¹⁰X. Duan, C. Niu, V. Sahi, J. Chen, J. W. Parce, S. Empedocles, and J. L. Goldman, *Nature (London)* **425**, 274 (2003).

¹¹Z. Zhong, Y. Fang, W. Lu, and C. M. Lieber, *Nano Lett.* **5**, 1143 (2005).

¹²Calculated by the work functions of *n*-type Si and Nickel. Data were adopted from S. M. Sze, *Physics of Semiconductor Devices*, 2nd Ed. (Wiley, New York, 1981).

¹³D. V. Averin and K. K. Likharev, *J. Low Temp. Phys.* **62**, 345 (1986).

¹⁴L. J. Geerligs, V. F. Anderegg, J. Romijn, and E. Mooij, *Phys. Rev. Lett.* **65**, 377 (1990).

¹⁵S. Tarucha, D. G. Austing, T. Honda, R. J. vd. Hage, and L. P. Kouwenhoven, *Phys. Rev. Lett.* **77**, 3613 (1996).

¹⁶S. Moriyama, T. Fuse, M. Suzuki, Y. Aoyagi, and K. Ishibashi, *Phys. Rev. Lett.* **94**, 186806 (2005).

¹⁷H. Van Houten and C. W. J. Beenakker, *Phys. Rev. Lett.* **63**, 1893 (1989).

¹⁸C. W. J. Beenakker, *Phys. Rev. B* **44**, 1646 (1991).